J. Earth Syst. Sci. (2021)130 166
https://doi.org/10.1007/s12040-021-01674-3

Heat wave characteristics over India during ENSO events

N Naveena[1], G Ch Satyanarayana[1,4,*], K Koteswara Rao[2], N Umakanth[1] and D Srinivas[3]

[1]*Department of ECE, Center for Atmospheric Science, K L Deemed to be University, Green Fields, Vaddeswaram, Andhra Pradesh 522 502, India.*
[2]*Centre for Climate Change and Sustainability, Azim Premji University, Bengaluru, India.*
[3]*National Centre for Medium Range Weather Forecasting, Ministry of Earth Sciences, A-50, Sector-62, Noida, India.*
[4]*Andhra Pradesh State Development and Planning Society (APSDPS), Govt. of AP, Vijayawada, Andhra Pradesh, India.*
**Corresponding author. e-mail: gcsatya@kluniversity.in*

MS received 26 September 2020; revised 14 February 2021; accepted 6 May 2021

El-Nino Southern Oscillation (ENSO) is a major ocean–atmospheric coupled phenomenon in the Tropical Pacific Ocean that influences the Indian summer-time temperatures during April and May. In the current analysis, we examined the impact of ENSO on Indian heat waves. Temperature zones are identified when the maximum temperature exceeds 42°C, particularly during April and May over the Indian subcontinent. The results depicted three different regions (west Rajasthan, northwest and southwest UP, and south-central India) that experienced the frequency in days with maximum temperature above 42°C. These means are compared with those of Preceding El Nino (PEN), El Nino (EN) and Succeeding El Nino (SEN) events. It is found that PEN and SEN years experienced high positive anomalies. It can be seen that an increase in surface temperatures and heat waves are closely associated with the strengthening of north-westerlies and reduction of geopotential height at 500 hPa level, reduction of soil moisture and increase of sea surface temperatures (SST) during PEN and SEN events. The results also show that the variations in temperature and heat waves over northeast India are different from the rest of India during EN and SEN years. The three maximum temperatures regions of (1) west Rajasthan, (2) east Uttar Pradesh, and (3) Vidarbha, are identified based on both the magnitude and frequency days of above 42°C maximum temperatures. The spectrum analysis is performed for the monthly time series of the days exceeding daily surface maximum temperature 42°C for the three regions and identified the dominant periodicities with 2.2–2.8 and 3.3–8.5 years, which could be endorsed to ENSO and QBO frequencies.

Keywords. ENSO; temperatures; heat waves; geopotential height; soil moisture.

Supplementary material pertaining to this article is available on the *Journal of Earth System Science* website (http://www.ias.ac.in/Journals/Journal_of_Earth_System_Science).

Published online: 14 August 2021

1. Introduction

Heat waves are the extreme events during the summer season, impact the Indian subcontinent significantly. From the mid-20th century, many parts of the country have been experiencing an augment in these events frequency and duration (Cowan *et al.* 2014). Extreme heat waves have large societal impacts, particularly, human illness, crop failures, wildfires, power outages, infrastructure disruption and damage (Garcia-Herrera 2010). Horton *et al.* (2016) mentioned that the heat waves are exacerbated due to the changing climatic conditions and have become one of the deadliest natural disasters in modern existence. Current observations recommend that the frequency, duration, and intensity of heat wave events are escalating over land regions across the globe (Coumou and Rahmstorf 2012). This alteration in heat wave characteristics mainly depends on the modest amounts of mean global warming associated with anthropogenic climate change (Coumou *et al.* 2013).

It is well acknowledged that ocean is the primary driver of climate variability and an essential source of increased summer temperature variability due to differential land and ocean warming, particularly from variations in circulation patterns or land surface/radiative fluxes (Bronimann 2007; Holmes *et al.* 2015). The local weather systems and climate of a region can be influenced by the anomalies of SST through the changes in the atmospheric flow patterns and also influenced by the remote effects, so called teleconnections. El Nino Southern Oscillation (ENSO) is linked with the sea surface variation in the equatorial Pacific Ocean, and plays a key role in the heat management on the global scale (Firpo *et al.* 2012; Newman *et al.* 2016). ENSO is a climate event (Ropelewski and Halpert 1987; Su *et al.* 2001), which influences the air temperature and precipitation variability in many regions all over the globe (Kushnir *et al.* 2010; Pezza *et al.* 2012; Rusticucci *et al.* 2012; Hoell *et al.* 2017; Ham 2018) in association with the changes in the SST anomalies (Bhalme *et al.* 1983; Rasmusson and Carpenter 1983; Kiladis and Diaz 1989; Halpert and Ropelewski 1992; Hastenrath and Heller 2006). The El Nino events have an important relationship with the extreme weather events over the globe (Wolter *et al.* 1999).

There were many studies regarding the tremendous temperature variations over India during summertime (Kothawale and Rupa Kumar 2005; Alexander *et al.* 2006; Rupa Kumar *et al.* 2006; Srivastava *et al.* 2009), but very few studies attempted in relation with El Nino events. Previous studies reported that the daytime and night-time temperatures are increasing over western Pacific and East Asia regions during the succeeding El Nino years (Nicholls *et al.* 2005). The Asian continent heat waves are associated with enhanced incoming solar radiation, decreased precipitation, and increased surface pressure, presence of low-level anticyclonic circulation (Lu and Chen *et al.* 2016). Strengthening of subtropical high in the Western North Pacific (WNP) acts as the main contributor to the development of heat waves in the Asian region (Luo and Lau 2017; Zeng *et al.* 2017). Mazdiyasni *et al.* (2017) reported that the mean temperatures over the Indian subcontinent increased by more than 0.5°C during 1960–2009, leading to a higher mortality rate. A significant correlation was observed in April–May between ENSO and aerosol loading which was particularly observed in the North Indian region (Kim *et al.* 2016). Chase *et al.* (2006) found that the natural variability of El Nino and volcanism may have greater importance than any general warming trend in causing extreme regional temperature anomalies. While soil moisture is imperative to understand heat wave development through land–atmosphere feedback, due to the lack of dense soil moisture observation networks in various parts of the world (including India), several studies have employed terrestrial water storage (TWS) observations to scrutinize heat waves (Andersen *et al.* 2005; Fischer *et al.* 2007; Hauser *et al.* 2016).

There is a significant enhancement in the length of heat wave days, frequency and intensity of heat waves over India and also the anomalies of SST over the Indian Ocean and El Nino events, Indian and Pacific Ocean effect heat wave occurrences over India (Rohini *et al.* 2016). Tropical Indian Ocean SSTs have been showing an increasing trend since the last half-century (Roxy *et al.* 2014, 2015). They will continue to increase in the future due to the aggregation of greenhouse gases and also in one of the study authors proposed that the average climatic condition of the tropical Pacific is estimated to vary in future because of warming induced due to greenhouse gases (Cai *et al.* 2015). Because of these changes, the frequency of extreme events such as El Nino increases and also, with an increase in the SSTs of the tropical Indian Ocean,

more intensified and more durable heat waves probably occur in the future over the Indian subcontinent.

Multiple studies suggest that maximum, minimum and mean temperatures over the Indian subcontinent are expected to increase in the future. Kothawale and Rupa Kumar (2005) identified a significant increase in annual mean temperature of about 0.05°C per decade during the period 1901–2003 and 0.22°C per decade during the period 1971–2003 over the Indian region. The highest intensity of heat waves was recorded in India during 2015, which took a death toll of nearly 2500 and 2320 human lives in Andhra Pradesh and Telangana states respectively (Dodla *et al.* 2017; Naveena *et al.* 2021b). India practiced a sequence of heat waves in the past and that exposes important mortality impacts. For example, the Orissa state (Odisha) faced an unprecedented heat wave situation in 1998 and around 2042 people lost their lives. In another case, during 2003 in Andhra Pradesh nearly 1421 people were dead and also nearly 1344 people were killed during 2010 in Ahmedabad city, India due to heat waves.

The main motivation for the study was taken from the research article by Pai *et al.* (2013). The present work has broadened our understanding of the influences of ENSO on temperature changes over India. This work focuses on examining the impacts of ENSO on various aspects of HW events, including frequency, duration, and amplitude, by analyzing observational records collected by a dense network of weather stations. We identified the temperature zones based on maximum temperature during the months of April and May over Indian subcontinent for this purpose. Here we made an attempt to show the heat wave characteristics such as the frequency, area of coverage and intensity of heat waves along with its associated synoptic features during Preceding El Nino (PEN), El Nino (EN) and Succeeding El Nino (SEN) years for the period 1951–2015 during the pre-monsoon season. This also implies classification of the vulnerable regions of heat waves, identifying the probable reasons by understanding the connections in terms of regional atmospheric flow variations. This study strives to enhance our understanding of HWs across India. This effort will also improve our skill in forecasting HW occurrences.

Moreover, existing studies mainly focused on extremely high temperatures rather than consecutive HW events. As the ENSO phenomena in the Pacific are known to impact weather and climate over various parts of the world, this phenomenon impact on the HWs during PEN, EN and SEN years over India was examined.

In the present analysis, we have examined the mortality rate due to heat waves during El Nino, along with the preceding and succeeding years and noticed that the death rate due to heat wave is higher during succeeding El Nino year when compared to El Nino and its preceding year as shown in table 2. The Indian subcontinent experiences heat waves during the summer months of April and May, but the highest intensity occurs in the month of May. We also analysed the spatial distribution of temperatures, frequencies in days when the daily maximum temperature exceeds above 42°C, and heat waves over the Indian subcontinent during April and May in different El Nino phases. The results are illustrated in section 3 in detail and are summarised in section 4.

2. Data and methodology

Daily maximum and minimum temperatures data for the period 1951–2015 at 1°×1° horizontal resolution for the Indian region (Srivastava *et al.* 2009) had been taken from India Meteorological Department (IMD). The monthly climatological means of maximum and minimum temperatures were calculated for April and May considering the 65-year study period at each grid point. Composite anomalies were computed for preceding El Nino (PEN), El Nino (EN) and succeeding El Nino (SEN) years. The El Nino years were identified based on the Oceanic Niño Index (ONI) and taken from the website https://ggweather.com/enso/oni.html and also listed in table 1. ONI was computed as a 3-month running mean of SST anomaly for the Niño 3.4 region (5°N–5°S, 120–170°W).

We calculated the number of days with maximum temperatures >42°C in April and May at each grid point to identify the extreme temperature zones.

The number of heat wave days were identified based on the IMD criteria used in many studies (De and Mukhopadhyay 1998; Chaudhury *et al.* 2000; Pai *et al.* 2004, 2013, 2017; Ray *et al.* 2013; Ratnam *et al.* 2016), which is as follows: (i) normal heat wave is confirmed if the maximum temperature at a station reaches ≥40°C for plains and ≥30°C for hilly regions, and the departure from normal is 4–6°C; (ii) severe heat wave is declared if the mean

Table 1. *List of El Nino years used in the study.*

Sl. no.	El-Nino type	Years
1	Moderate	1951, 1963, 1968, 1986, 1994, 2002, 2009
2	Strong	1957, 1965, 1972, 1987, 1991
3	Very strong	1982, 1997

maximum temperature is ≥40°C and temperature departure from normal is above 6°C or if the actual maximum temperature is ≥47°C or if the actual maximum temperature is ≥6.5°C above normal; and (iii) over the coastal stations, the heat wave is declared if the maximum temperature exceeds 37°C along with departure from normal is ≥4°C. Additionally, the existence of heatwaves is established only if the criteria of heat wave continue for at least 3 days constantly. The filtered time series were then applied to spectrum analysis using maximum entropy methods (Barrodale and Erickson 1978).

NCEP (National Centres for Environmental Prediction)/NCAR (National Centre for Atmospheric Research) Reanalysis-1 global analysis monthly mean data at 2.5° spatial resolution was used to compute mean composite anomalies of zonal wind at 925 hPa, geopotential height at 500 hPa and soil moisture for PEN, EN and SEN years during 1951–2015 (http://www.esrl.noaa.gov/psd/data/gridded/data.ncep.reanalysis.html).

And also in our present analysis, a new methodology called percentile method was adopted. 90th and 95th percentile of maximum temperature for PEN, EN and SEN years in the study period for April and May months using IMD gridded data was performed. This method is often used to calculate temperature extremes usually ranging from 90th to 99th percentile (Alexander *et al.* 2006; Moberg *et al.* 2006; Fischer and Schar 2008, 2010; Lhotka and Kysely 2015; Hoy *et al.* 2017). The choice of selecting percentile is very important such as 99th percentile enhances the chance of the identification of the events probably creating serious threat to environment and society, but the frequency of happening of such events create an amount of improbability due to scarcity (Zhang *et al.* 2011). Hence by considering all these aspects, 90th and 95th percentile were chosen for the present analysis.

Further, the monthly SST data was archived from NOAA extended reconstructed sea surface temperature (SST) V4 for April and May during 1951–2015 (http://www.esrl.noaa.gov/psd/data/gridded/data.noaa.ersst.html).

3. Results and discussion

In the present study, we analysed the heat wave characteristics and their associated synoptic features in PEN, EN and SEN years for the period 1951–2015. We compared the heat wave induced mortality rate during PEN, EN and SEN years and were shown in table 2 and this data was obtained from the India Meteorological Department.

3.1 *Mean maximum and minimum temperature*

Climatological features of surface maximum and minimum temperatures during April and May were shown in figure 1. In April (figure 1a), the highest mean maximum temperature around 40°C was observed over Vidarbha region and a broad belt of high temperatures of about 38°–40°C were observed over north and south-central India. In contrast, rest of the country experienced around 38°C. An increase in the intensity of temperatures was noted during May (figure 1b) and most parts of India were experiencing the highest intensity of heat waves during this month. Maximum temperatures above 40°C extend from west Rajasthan to coastal Andhra Pradesh region passing through west and east Rajasthan as well as southern parts of west and east Uttar Pradesh (UP), Madhya Pradesh, Vidarbha and Telangana during this month. The highest temperatures above 42°C were recorded over the south-central parts of Vidarbha and northwest Madhya Pradesh regions. It is vital to note that the maximum temperature over west Rajasthan, a desert climate (sandy soil) region, is at least one to two degrees lower than over north and central parts of India. This clearly shows that May month is the representative month for highest temperatures over the Indian subcontinent. Along with this, we also studied the behaviour of minimum temperatures during these months. During April, the minimum temperatures above 24°C were observed in the east coastal region, Telangana and south Vidarbha (figure 1c). Around 22–24°C were observed in some parts of Gujarat, Saurashtra, Kutch & Diu, Konkan & Goa, Madhya Pradesh

Table 2. *Mortality rate and heat wave days during PEN, EN and SEN years.*

PEN year			EN Year			SEN Year		
Year	No. of HW	Deaths	Year	No. of HW	Deaths	Year	No. of HW	Deaths
1981	6.17	75	1982	6.22	0	1983	10.95	185
1986	6.51	156	1987	8.188	91	1988	9.66	627
1993	8.65	42	1994	7.82	234	1995	11.53	413
1996	6.81	26	1997	7.58	21	1998	18.17	1655
2001	6.20	70	2002	8.44	909	2003	13.15	1494
2008	4.22	616	2009	9.27	1071	2010		1274

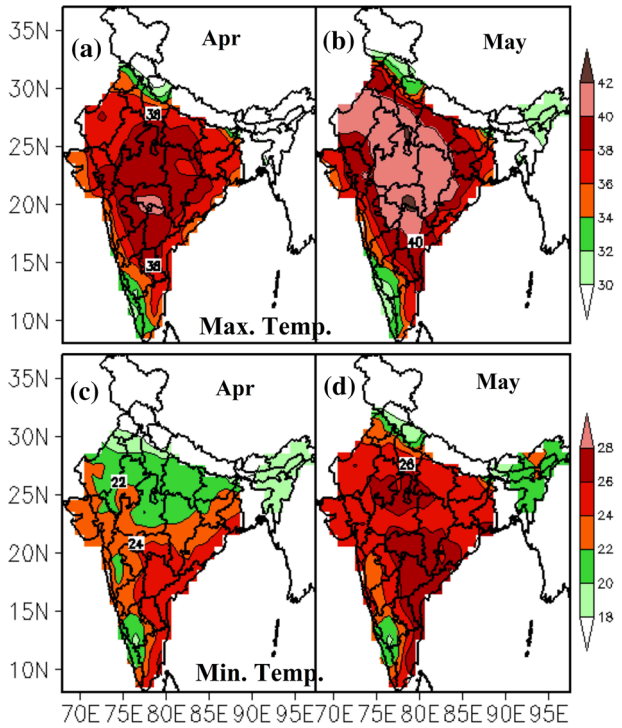

Figure 1. Spatial distribution of mean temperature (upper panel) maximum **(a, b)**; (lower panel) minimum **(c, d)** during the period 1951–2015 for April and May.

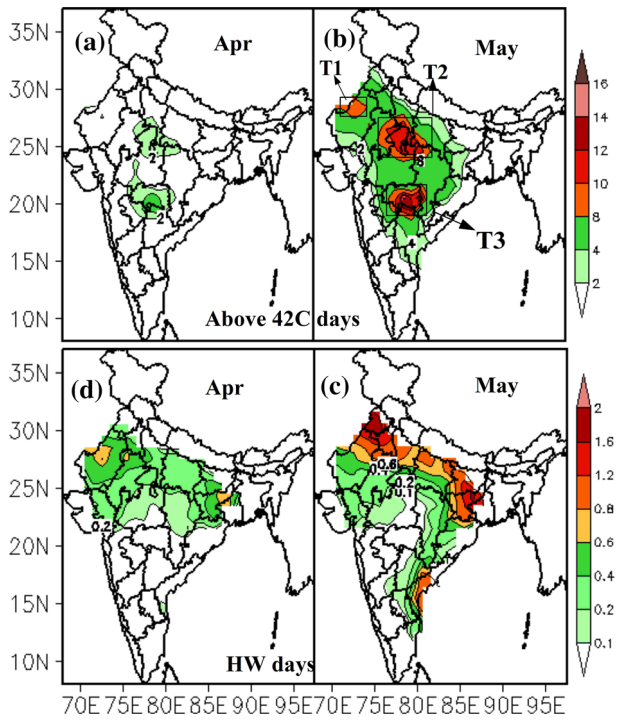

Figure 2. Spatial distribution of mean maximum temperature frequencies of (upper panel) above 42°C days **(a, b)**; (lower Panel) mean temperatures >40°C and anomalies above 4°C days/year **(c, d)** from 1951 to 2015 for April and May.

and southern parts of Chhattisgarh. The mean minimum temperatures were also showing an increasing tendency in May. There are two distinct regions of temperatures exceeding 26°C, which are in east-central parts of India (Telangana, Andhra Pradesh, Vidarbha, the southern part of Chhattisgarh and Orissa) and north-central parts of India (east Rajasthan, west and east Madhya Pradesh, east UP) (figure 1d).

3.2 *Frequency of days above 42°C days and heat wave days*

The number of days with maximum temperatures exceeding 42°C is computed and presented in figure 2(a and b) during the period 1951–2015. In April, the frequencies of heat wave days above 42°C are less and it is about 2 days over northwest Madhya Pradesh (MP) and southwest Uttar Pradesh, and east Maharashtra (figure 2a) (Satyanarayana and Dodla 2020; Naveena *et al.* 2021a). During May, the spatial distribution shows that the higher frequency regions are consistent with the areas of maximum temperature. It is identified that the occurrence of heat waves are more in the regions of west Rajasthan (T1), northwest Madhya Pradesh (T2) and southwest Uttar Pradesh (T3), and east Maharashtra (figure 2b). The highest frequencies of about 10 days per month are noted in three regions, whereas west

Rajasthan experiences the frequency of about 8–10 days. The frequencies of about 2–8 days are observed over north and south-central parts of India. The spatial distribution of maximum temperatures and the frequencies clearly indicate the three regions extending from northwest to north-central and further to south-central parts of India are the hottest zones compared to the rest of the Indian subcontinent and are clearly distinguishable. It is clearly seen in figure 2(b), that the three distinct isolated hotspots are important identifications that would be useful to understand the occurrence of heat waves.

The climatological mean of frequency of days above 42°C was also plotted from January to December individually for the study period as given in the supplementary section. The days with temperatures above 42°C were observed only during April, May and June. The description for the days with temperature above 42°C for April and May are given above. In June, highest intensity was observed over NW and north-central India of the order of 6–12 days as the hot season in southern India is finished by the initial days of June with the onset of summer monsoon, whereas it ends by early July in the northern India. No days with frequency above 42°C were observed in the remaining months.

Following the heat wave definition by the IMD as given in section 2, the spatial distribution of the number of days with the maximum temperature exceeding 40°C and their deviation is higher than 4°C during April and May are shown in figure 2(c and d). In the month of April, a very less number of heat waves (0.8 days/year) occurred over west Rajasthan and northeast India (figure 2d), whereas in May, the distribution of frequencies shows a broad region extending from northwest part towards northeast up to the West Bengal and extending southwards covering the southeast coastal regions (figure 2c). This resembles a 'comma' pattern and with the northern and eastern parts having higher frequencies than the southern parts, except a small region over southeast (coastal AP). Although it is easier to understand higher frequencies over the north, the maximum over southeast India is an important feature that has been further investigated.

3.3 *Periodicities of above 42°C maximum temperature days*

Using the maximum entropy method, we obtained the power spectra of maximum temperatures days (above 42°C days) of May during 1951–2015 (figure 3). The power spectra indicate that predominant power is confined to frequencies with periods ranging from 2.0 to 12.8 years. Therefore, the periods are divided into four categories: 2.0–2.5 years, 2.6–3.5 years, 3.6–8.0 years and greater than 8.0 years. It clearly shows that the Vidarbha region exhibits 2.46 years, 4.57 years periodicities, whereas Rajasthan and east UP are exhibiting the periodicities of 2, 3.6, 4.9 and 8 years. Generally, 2.4–2.7 years periodicity is attributed to QBO, 3.3–8.4 years periodicity is attributed to ENSO. The 2.0–3.0 years periodicities have been reported by many of the earlier studies (Parthasaradhy and Dhar 1974; Webster *et al.* 1998) and may be attributed to the quasi-biennial oscillation (QBO). The significant 3–8 years periodicities may be attributed to El-Nino Southern Oscillation (ENSO) (Trenberth 1976; Philander 1983; Webster *et al.* 1998). From the above periodicities, the effect of quasi-biennial oscillation and ENSO are more on May month maximum temperatures and days exceeding 42°C over India.

3.4 *Composite anomaly of mean maximum temperature*

We estimate the composite anomalies of mean maximum temperatures during the three phases of El Nino, i.e., preceding El Nino (PEN), El Nino (EN) and succeeding El Nino (SEN) years. In April, during the EN years, negative anomalies are observed all over India indicating the cool phase (figure 4b), whereas positive anomalies are shown during the SEN years leading to the warm phase (figure 4c). During PEN years, positive anomalies are shown over northwest and northeast India and negative anomalies remaining parts of India (figure 4a). Similarly, in May during PEN years (figure 4d), southern parts of India show positive anomalies, EN years central northeast India (Gangetic West Bengal, Jharkhand, Bihar, Sub-Himalaya, West Bengal). Parts of northeast India show positive anomalies (figure 4e), and during SEN years all parts of India except central northeast and northeast regions show positive anomalies (figure 4f). From this analysis, it is evident that El Nino plays a major role in the occurrence of the heat waves over India and the shifting of heating region. From this analysis, during SEN years in both April and May India experiences warmer temperatures and cooler during EN years.

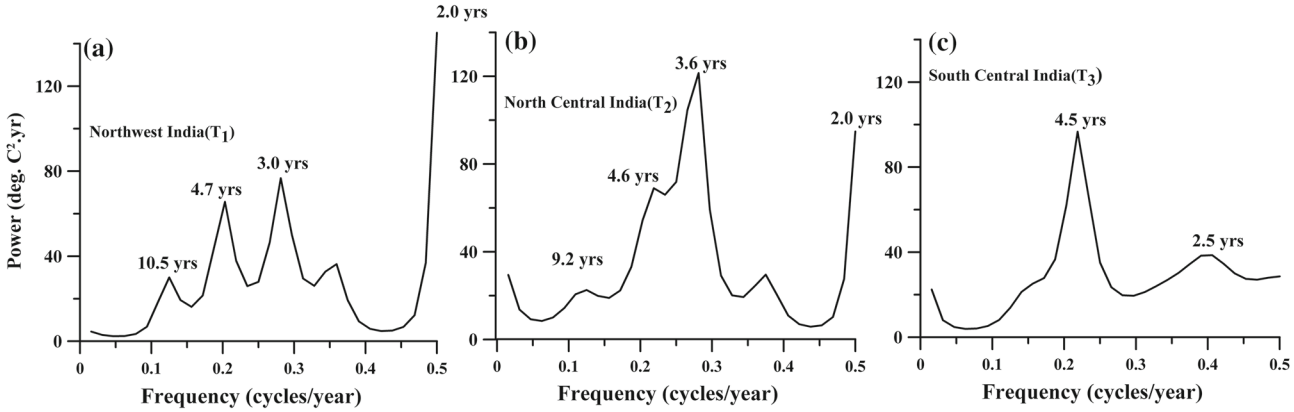

Figure 3. Power spectra of number of days maximum temperatures exceeding above 42°C over **(a)** northwest India; **(b)** north-central India, and **(c)** south-central India for the period 1951–2015 using maximum entropy method.

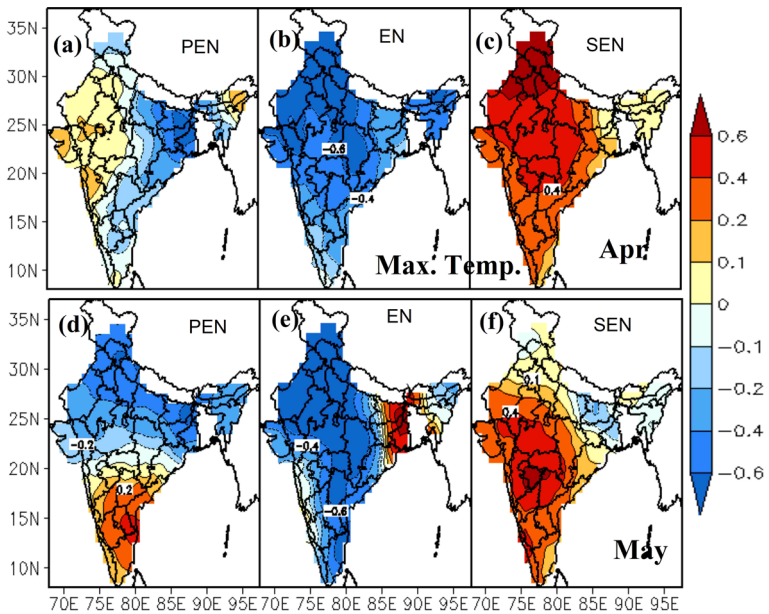

Figure 4. Composite anomalies of mean maximum temperatures during PEN, EN and SEN for April (upper panel, **a–c**) and May (lower panel, **d–f**) from 1951 to 2015.

3.5 *Composite anomaly of mean minimum temperature*

Spatial patterns of mean minimum temperatures during PEN, EN, and SEN years for April and May are presented in figure 5. These features are similar to maximum mean temperatures as described in section 3.4. During PEN years, northwest and parts of southern India show positive anomalies in April (figure 5a), whereas south peninsular India regions are warmer in May (figure 5d). During EN years, April and May show a cold phase as directed for maximum temperatures (figure 5b, d). During SEN years, April and May show a warming phase over the Indian region (figure 5c, f). The spatial distribution of minimum temperature anomalies clearly indicates the warm phase during the SEN years and the cool phase during the EN years all over India for both April and May months.

3.6 *Composite anomaly of frequency of days above 42°C*

Composite anomalies of the frequency of days exceeding maximum temperature above 42°C are analysed and presented in figure 6. The figure depicts the spatial patterns similar to maximum temperature (figure 4). During EN years, both April and May show negative anomalies, show cooling period (figures 6b, e) in almost 70% of the Indian region. During PEN years, positive

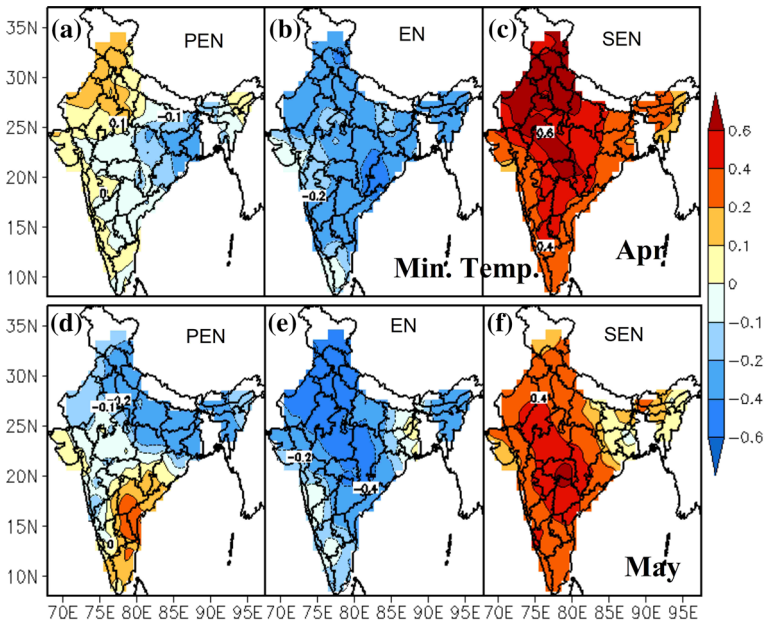

Figure 5. Composite anomalies of mean minimum temperatures during PEN, EN and SEN for April (upper panel, **a–c**) and May (lower panel, **d–f**) from 1951 to 2015.

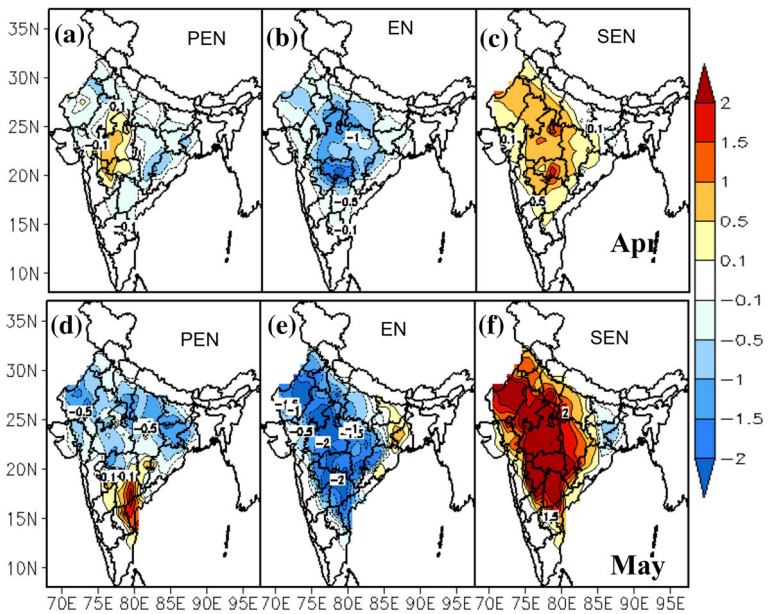

Figure 6. Composite anomalies of frequency of days above 42°C during PEN, EN and SEN for April **(a–c)** and May **(d–f)** from 1951 to 2015.

anomalies are observed over central India during April and over parts of southern coastal regions (AP and Telangana) during May (figure 6a, d). Positive anomalies are noted during PEN years in most parts of the country (figure 6c, f). This analysis shows that frequency of days above 42°C is more during SEN years both in April and May and contributing to maximum temperatures over most parts of the country.

3.7 *Composite anomaly of heat wave days*

Figure 7 shows the composite anomalies of the number of days with the mean maximum temperature exceeding 40°C along with more than the mean+4°C days corresponding to PEN, EN and SEN years for April (top panel) and May (bottom panel). The spatial distribution of composite anomalies shows positive in SEN

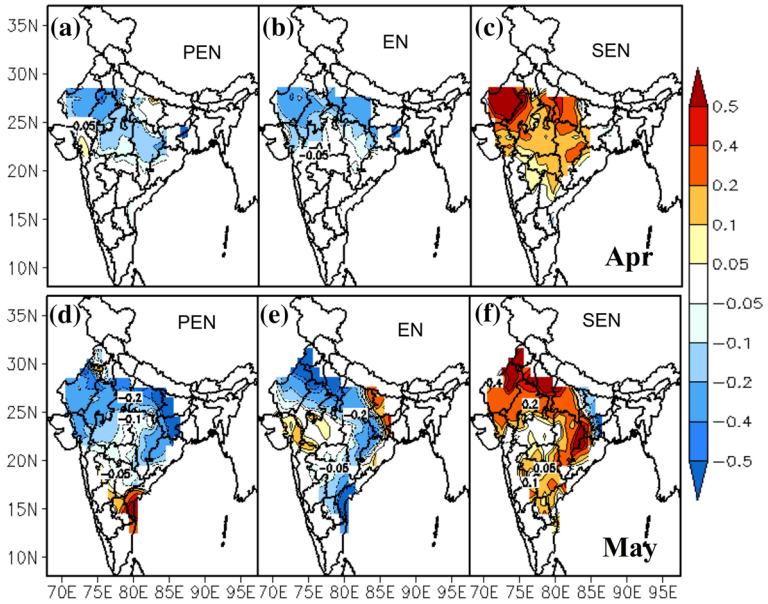

Figure 7. Composite anomalies of heat wave days (mean+4°C) during PEN, EN and SEN for April **(a–c)** and May **(d–f)** from 1951 to 2015.

years in April and May months in most of the parts of the country (figure 7c, f), whereas negative during EN years (figure 7b, e). During PEN years, negative anomalies (figure 7a) during April and positive anomalies over AP region kept remaining regions negative in May (figure 7d). Finally, we understood that most parts of India warmer during PEN years and cooler during EN years during April and May, but these anomalies having a higher magnitude in May.

In recent years, the influence of El Nino is more brutal due to the global warming and leads to deteriorating the situation as the temperatures continuously increase. This analysis also proposes that the increase in the number of heat waves is mostly governed by the rise in temperature due to anthropogenic emissions of GHGs.

3.8 *Composite anomalies of maximum temperature for 90th and 95th percentile for April and May*

The spatial distribution plot of the anomaly of 90th and 95th percentile of the daily maximum temperature for the study period for April and May months have been plotted. These percentiles are significant statistical tools that specify the characteristics of temperature changes. These anomalies of 90th and 95th percentile during the PEN, EN and SEN indicate the characteristics of temperature represent the features in that perspective mode of climate. For the 90th percentile in April during PEN, negative anomalies were observed all over the Indian subcontinent except over a small region of north-western Madhya Pradesh indicating a decrease in temperatures during PEN years (figure 8a–c). During El Nino years all over the Indian subcontinent is occupied with negative anomalies of 90th percentile except over northeastern part of the country. During SEN years in April, higher intensity of positive anomalies was observed excluding few parts over northeastern and southeast coast India. In May, characteristic features of temperature were observed clearly during PEN, EN and EN (figure 8d–f). During PEN, only southeast coastal parts were warmer and in EN years, the northeastern India is warmer and remaining country is cooler, whereas in SEN years complete India is warmer except NE India. Similar phenomenon was observed for 95th percentile but with a lesser intensity of anomalies as shown in figure 9.

3.9 *Anomalies of zonal wind and geopotential height at 500 hPa for May month*

To classify the large-scale mechanisms occupied with Indian heat waves, we studied the large-scale atmospheric circulation patterns during the heat wave periods. ENSO is influencing the occurrence of heat waves due to the Walker circulation shift over the Pacific Ocean. Our analysis showed this

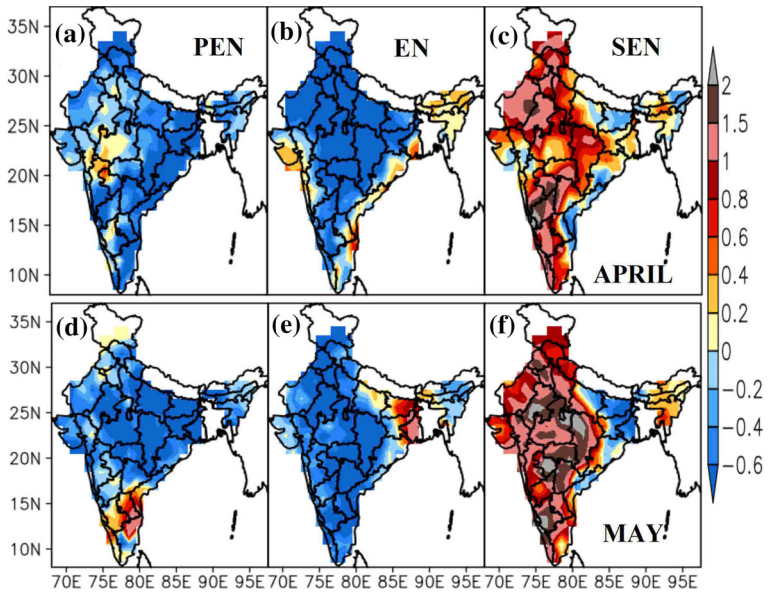

Figure 8. 90th percentile of maximum temperatures during PEN, EN and SEN for April and May during 1951–2015.

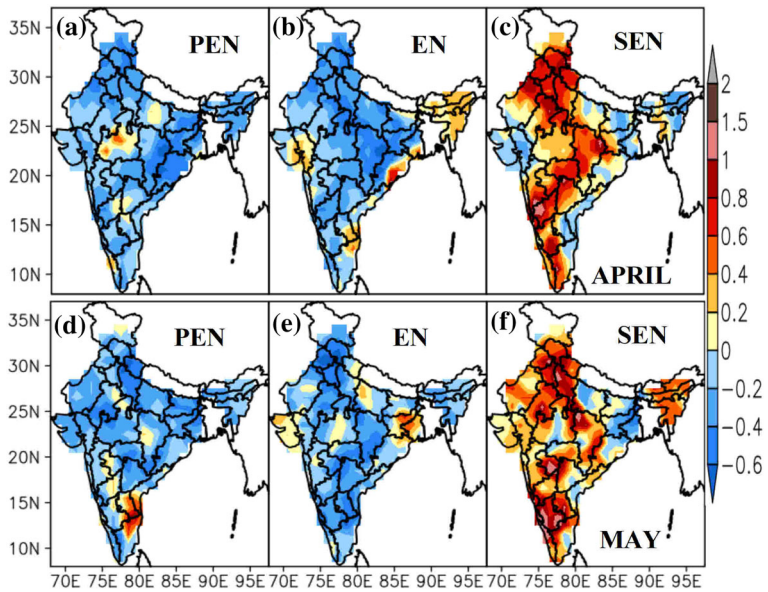

Figure 9. 95th percentile of maximum temperatures during PEN, EN and SEN for April and May during 1951–2015.

with the geopotential and wind anomalies and soil moisture at the surface level. Atmospheric circulation is one of the most critical factors influencing weather and climate conditions, including extreme events. An increase in atmospheric circulation stability is considered one of the main factors explaining the more frequent extreme air temperatures in India.

Ratnam *et al.* (2016) and Rohini *et al.* (2016) were discussed the processes maintaining the heatwaves over India, particularly on the atmospheric circulation patterns. However, their articles main objective is to define atmospheric circulation conducive to the occurrence of heat waves, which is an important issue and gives a chance to explain the origins of these extreme events. Specific types of pressure patterns at sea level and at the geopotential height of 500 hPa, which lead to extreme air temperature values, are distinguished and characterized. To find out the pressure and thermal conditions in the middle and higher troposphere accompanying heat waves, the vertical structure of geopotential height anomalies and corresponding anomalies of air temperature at an appropriate geopotential height during the episodes of surface highest temperature are

identified and described. Recognizing the circulation patterns governing the occurrence and duration of heat waves may help to forecast these events.

Here, we have analysed the mean zonal wind and geopotential height (GPH) anomalies at 500 hPa during PEN, EN and SEN years over the south Asia region for the month of May and are presented in figure 10. The spatial distribution of mean zonal wind anomalies at 925 hPa during PEN years shows negative anomalies over north and north-eastern parts of India, and positive anomalies over northwest and southern parts of India (figure 10a). During EN years, positive anomalies are observed in north-eastern parts of India and maximum core region is observed in Bihar, West Bengal (0.6 m/s), whereas negative anomalies over the northwest and southern parts of India along with maximum value seen over the southeast coastal regions (figure 10b). Therefore more heat waves occur over northeast India during El Nino years because of increasing of westerlies. The westerlies from northwest, i.e., from southern parts of Middle East and southwest, i.e., from Oman coast brings hot air resulting in the advection of hotter air that supplements the seasonal heating during pre-monsoon season (Yadav 2016).

In SEN years, the negative anomalies dominated over southern and north-western parts of India. However, the positive anomalies are shown all over the northwest and southern parts of India. It is observed that the maximum positive values concentrated over north-western parts of India during this period. Hence, the positive anomalies indicate the westerlies are more strengthening during SEN years (figure 10c).

The 500-hPa GPH anomaly shows the negative anomalies during PEN years over many parts of the country (figure 10d). In EN years, the maximum negative anomalies observed over the Indian subcontinent except over southern India occupied with positive anomalies with minimum values of 0–2 (figure 10e). During SEN years, positive anomalies are observed all over the country (figure 10f). These positive anomalies in GPH suggest that large-scale circulation patterns linked with high temperature conditions.

From this, we noticed the strengthening of geopotential height due to the increase of clear sky days, associated with higher pressure might be one of the reasons for increase in surface temperatures and intensified heat waves during preceding and succeeding El Nino years.

A positive anomaly in 500-hPa GPH indicates a clear sky that is associated with conditions such as air subsidence, generation of light wind movements and warm air advection, and results in prolonged hot conditions at the surface (Meehl and Tebaldi 2004).

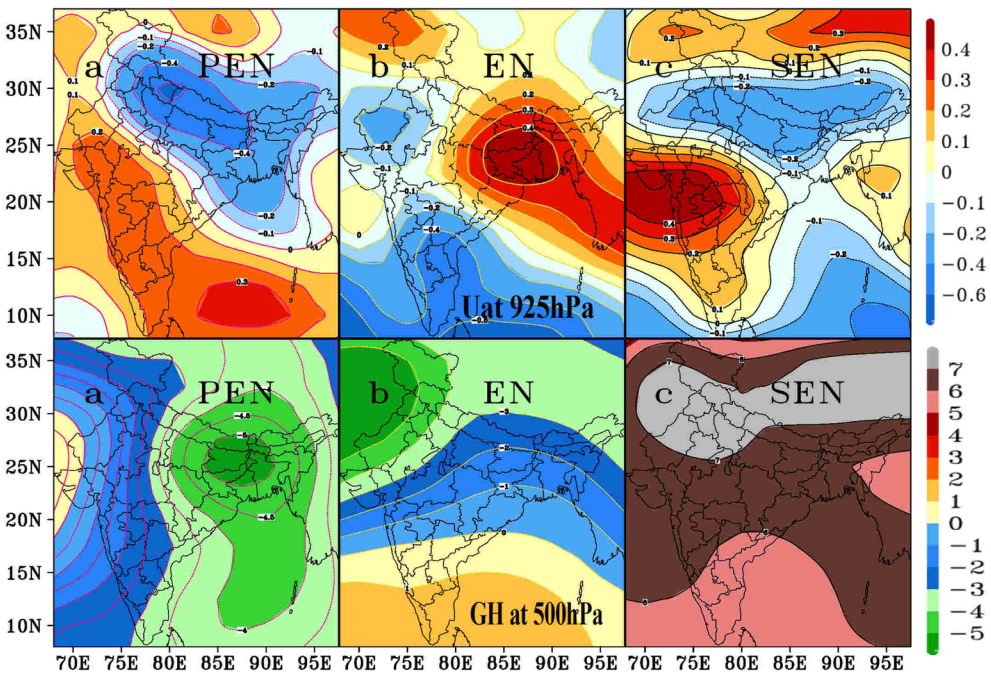

Figure 10. Composite anomalies of zonal wind at 925 hPa (upper panel) and geopotential height at 500 hPa (lower panel) during PEN, EN and SEN for May month from 1951 to 2015.

3.10 *Composite anomalies of soil moisture for May*

Previous studies found that summertime temperatures to be affected by soil moisture, depend on spring precipitation (Della-Marta *et al.* 2007; Fischer *et al.* 2007). The soil moisture variability is vital to comprehend the temperature changes through land–atmosphere feedback (Andersen *et al.* 2005; Fischer *et al.* 2007; Hauser *et al.* 2016). Sandeep and Prasad (2018) reported a strong correlation between the maximum temperature and soil moisture (−0.56), which indicates that soil moisture regulates the heat waves over India. The mean soil moisture anomalies are computed during PEN, EN, and SEN years in May which are shown in figure 11. The positive anomalies are observed over Telangana, coastal Andhra Pradesh, Orissa, Vidarbha, Bihar, eastern UP, Gangetic West Bengal and Jharkhand, whereas the rest of the country prevailing with negative anomalies (figure 11a) during PEN years. During EN years, the whole Indian subcontinent is shown with positive anomalies (figure 11b). During SEN years, except north-eastern parts, the rest of the country is occupied with negative anomalies (figure 11c). The negative anomalies of soil moisture are the triggering factor for increasing surface temperature during summer which leads to the occurrence of heat waves most predominantly in SEN years.

3.11 *Composite anomalies of sea surface temperature for April and May*

It is well known that the oceans are major drivers of internal climate variability, affecting climate around the globe. Many climatic variability modes are coupled ocean–atmosphere phenomena, such as the El Niño-Southern Oscillation (ENSO), which is the most essential mode of variability for global climate on inter-annual timescales. An El Niño episode affects many regions worldwide through atmospheric teleconnections and increases global average temperatures in that year. ENSO also affects temperature extremes in many regions across the world. SSTs can also be necessary for regional climate. Regionally, significant correlations between SST-driven runs and observations were mainly found in the tropics.

The spatial variation in sea surface temperature (SST) was observed over the Indian Ocean during PEN, EN and SEN years for 1951–2015 during April and May. Composite anomalies of SST

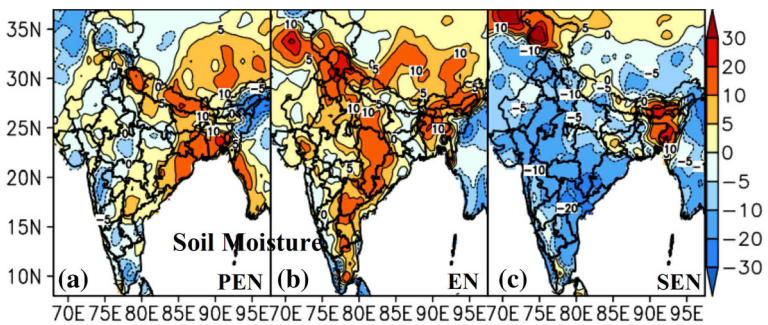

Figure 11. Composite anomalies of soil moisture during PEN, EN and SEN for May **(a–c)** from 1951 to 2015.

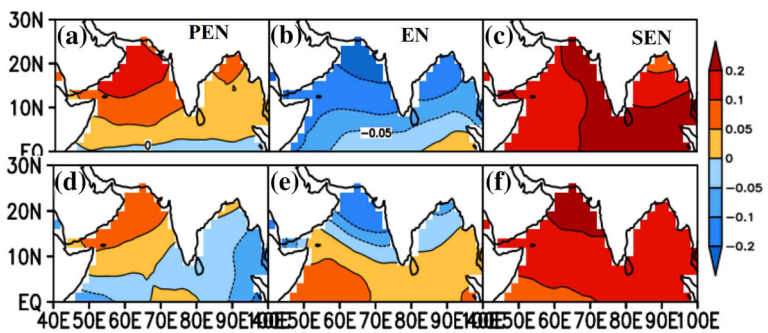

Figure 12. Spatial distribution of mean sea surface temperatures anomalies (upper panel) April, (lower Panel) May for the period 1951–2015 (**a**, **d**) PEN; (**b**, **e**) EN; (**c**, **f**) SEN.

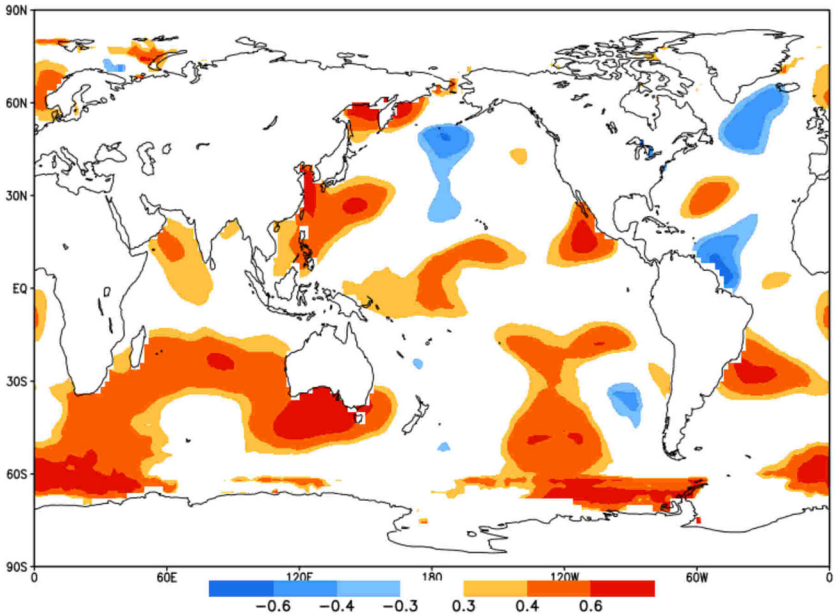

Figure 13. Temporal correlation between sea surface temperature and heat wave zone 3 maximum temperatures for the period 1951–2015.

during PEN (EN) in April indicates that both the Arabian Sea and Bay of Bengal have positive (negative) anomalies. In contrast, southwest and southeast Indian Ocean have negative (positive) anomalies as given in figure 12(a and b). During SEN, the whole Indian Ocean is occupied with positive anomalies (figure 12c).

In May, almost similar phenomenon is observed during PEN (figure 12d), whereas the rates of anomaly enhance during EN (figure 12e) and decrease during SEN (figure 12f) with respect to the April month SST anomalies. The robust positive relation between heat wave features and warming sea surface temperature (SST) indicates that the association of heat wave with SST anomalies and whole Indian Ocean has positive SST anomalies.

3.12 *Temporal correlation between sea surface temperature and heat wave zone 3 maximum temperatures*

We have prepared the correlation map of heat waves with that of the global SSTs to understand what other ocean basins are important for the heat wave occurrence and ENSO. Satyanarayana and Dodla (2020) identified three heat wave zones that are vulnerable to heat wave. Among these three zones, the highest recorded death rate due to heat wave was over zone 3 (HW3) and the regions come under this zone are Andhra Pradesh and Telangana. Global mean monthly sea surface temperature data for the period 1951–2015 during May and maximum temperature data for HW3 for the same period is taken and temporal correlation was seen. These two parameters are positively correlated and a positive correlation of about 0.4–0.6 was observed over West Indian Ocean. Central and western Pacific Ocean is also positively correlated. May month maximum temperatures over HW3 were positively correlated with SST gridded to generate a map presenting the SST-maximum temperature connotation at a global scale (figure 13). Furthermore, around the global ocean, significant correlations were observed over the western tropical Indian Ocean, eastern and western tropical Pacific Ocean, signifying these two oceans' imperative role in manipulating maximum temperature in the HW3. The spatial distribution of correlation coefficients recommends that the May temperatures in the HW3 were closely connected to the El Nino (Eastern Pacific SST anomalies near South American coast). Hence few areas were recognized which has a strong connection for maximum temperature in the HW3 during May.

4. Conclusions

This study investigates the heat wave characteristics during PEN, EN and SEN events using daily maximum and minimum temperature gridded data from IMD. The intensity, duration, frequency and

area of extent of heat waves and how do they vary during PEN, EN and SEN years are also carried out. Some of the important findings of this study include:

- The climatological mean of maximum temperature is evident that the maximum temperatures are higher than 1–2°C over north and central parts of India with respect to west Rajasthan.
- The frequency of heat waves with above 42°C gives a clear identification of the three isolated hotspot regions, namely northwest Madhya Pradesh, southwest Uttar Pradesh and east Maharashtra (Satyanarayana and Dodla 2020).
- The frequency of heat wave days with climatological mean+4°C is maximum during May over the southeastern parts.
- It was observed that heat wave events during SEN years intensify compared with the events during EN and PEN years. Also, the duration of heat wave events extends (shorten) during SEN (EN and PEN) over many parts of Indian subcontinent.
- The composite anomalies of mean maximum temperature, the frequency of days above 42°C and heat wave (>40°C and mean+4°C) days are higher than normal during SEN and cool during EN years all over the Indian subcontinent. Still, over northeast India reverse phenomena is observed.
- Composite analysis of minimum temperature is higher than the normal during SEN and lower during EN years. Also during PEN, minimum temperatures and heat wave days were higher over south-eastern parts of the country.
- Observed the synoptic features associated with heat waves during PEN, EN, and SEN from composite anomalies of zonal wind at 925 hPa, and it is evident that westerlies strengthen in SEN over the Indian subcontinent except over northeast India, which is the reason for the occurrence of more heat waves over these regions. Soil moisture anomalies regulate India's heat waves, which mean that maximum temperatures increase when soil moisture decreases and vice versa.
- Positive anomalies of SST are associated with warm temperatures over the Bay of Bengal and the Arabian Sea during PEN and SEN years.

The above results indicate that the observed QBO and ENSO phenomenon clearly reflects the above 42°C days and heat wave frequencies over India. It might be interesting to explore the periodicities of the surface maximum temperatures.

Acknowledgements

Part of this research is funded by SERB, Govt. of India under Grant No. ECRA/2016/001295. The authors acknowledge free data from European Centre for Medium-Range Weather Forecasts, India Meteorological Department, and NCEP/NCAR Reanalysis. This research is supported by Early Career Research Award, Science and Engineering Research Board, Government of India through financial support under Grant No. ECR/2016/001295.

Author statement

NN: Data collection, visualization, and draft preparation. GChS: Conceptualization, problem envision, methodology adoption, computation, software, visualization, data curation, validation, draft preparation and writing. KKR: Draft correction and editing. DS: Analysis and visualization. NU: Data collection and visualization.

References

Alexander L V, Zhang X, Peterson T C, Caesar J, Gleason B, Tank A K *et al.* 2006 Global observed changes in daily climate extremes of temperature and precipitation; *J. Geophys. Res.*, **111**, https://doi.org/10.1029/2005JD006290.

Andersen O B, Seneviratne S I, Hinderer J and Viterbo P 2005 GRACE derived terrestrial water storage depletion associated with the 2003 European heat wave; *Geophys. Res. Lett.* **32(18)** L18405, https://doi.org/10.1029/2005GL023574.

Barrodale I and Erickson R 1978 Algorithms for least-squares linear prediction and maximum entropy spectral analysis. Part I: Theory; *Geophysics* **45** 420–432, https://doi.org/10.1190/1.1441091.

Bhalme H N, Mooley D A and Jadhav S K 1983 Fluctuations in the drought/flood area over India and relationships with the southern oscillation; *Mon. Weather Rev.* **111** 8694, https://doi.org/10.1175/1520-0493(1983)111%3c0086:FITDAO%3e2.0.CO;2.

Brionnimann S 2007 Impact of El Nino-Southern Oscillation on European climate; *Rev. Geophys.* **45** 3, https://doi.org/10.1029/2006RG000199.

Cai W, Santoso A, Wang G *et al.* 2015 ENSO and greenhouse warming; *Nat. Clim. Change* **5** 849–859, https://doi.org/10.1038/nclimate2743.

Chase T N, Wolter K, Roger A, Pielke Sr and Rasool I 2006 Was the 2003 European summer heat wave unusual in a global context?; *Geophys. Res. Lett.* **3** L23709, https://doi.org/10.1029/2006GL027470.

Chaudhury S K, Gore J M and Sinha Ray K C 2000 Impact of heat waves over India; *Curr. Sci.* **79** 153–155, https://www.jstor.org/stable/24103439.

Coumou D, Robinson A and Rahmstorf S 2013 Global increase in record-breaking monthly-mean temperatures; *Clim. Change* **118**(3–4) 771–782, https://doi.org/10.1007/s10584-012-0668-1.

Coumou D and Rahmstorf S 2012 A decade of weather extremes; *Nat. Clim. Change* **2** 491–496, https://doi.org/10.1038/nclimate1452.

Cowan T, Purich A, Perkins S, Pezza A, Boschat G and Sadler K 2014 More frequent, longer, and hotter heat waves for Australia in the twenty-first century; *J. Clim.* **27** 5851–5871, https://doi.org/10.1175/JCLI-D-14-00092.1.

De U S and Mukhopadhyay R K 1998 Severe heat wave over the Indian subcontinent in 1998, in perspective of global climate 1998; *Curr. Sci.* **75** 1308–1311, https://www.jstor.org/stable/24101015.

Della-Marta P M, Haylock M R, Luterbacher J and Wanner J 2007 Doubled length of western European summer heat waves since 1880; *J. Geophys. Res.* **112** D15103, https://doi.org/10.1029/2007JD008510.

Dodla V B, Satyanarayana G C and Desamsetti S 2017 Analysis and prediction of a catastrophic Indian coastal heat wave of 2015; *Nat. Hazards* **87** 395–414, https://doi.org/10.1007/s11069-017-2769-7.

Firpo M A F, Sansigolo C A and Assis S V 2012 Climatology and seasonal variability of the number of warm and cold waves in Rio Grande do Sul associated to ENOS; *Rev. Bras Meteorol.* **27** 95–106, https://doi.org/10.1590/S0102-77862012000100010.

Fischer E M, Seneviratne S I, Vidale P L, Luthi D and Schar C 2007 Soil moisture–atmosphere interactions during the 2003 European Summer heat wave; *J. Clim.* **20** 5081–5099, https://doi.org/10.1175/JCLI4288.1.

Fischer E and Schar C 2008 Future changes in daily summer temperature variability: Driving processes and role for temperature extremes; *Clim. Dyn.* **33** 917–935, https://doi.org/10.1007/s00382-008-0473-8.

Fischer E M and Schar C 2010 Consistent geographical patterns of changes in high-impact European heatwaves; *Nat. Geosci.* **3** 398–403, https://doi.org/10.1038/ngeo866.

Garcia-Herrera R, Díaz J, Trigo R M, Luterbacher J and Ficher E 2010 A review of the European summer heat wave of 2003; *Crit. Rev. Environ. Sci. Technol.* **40** 267–306, https://doi.org/10.1080/10643380802238137.

Halpert M S and Ropelewski C F 1992 Surface temperature patterns associated with the southern oscillation; *J. Clim.* **5** 577–593, https://doi.org/10.1175/1520-0442(1992)005%3c0577:STPAWT%3e2.0.CO;2.

Ham Y G 2018 El Niño events will intensify under global warming; *Nature* **564(7735)** 192–193, https://doi.org/10.1038/d41586-018-07638-w.

Hastenrath S and Heller L 2006 Dynamics of climatic hazards in Northeast Brazil; *Quart. J. Roy. Meteorol. Soc.* **103** 77–92, https://doi.org/10.1002/qj.49710343505.

Hauser M, Orth R and Seneviratne S 2016 Role of soil moisture vs. recent climate change for the 2010 heat wave in western Russia; *Geophys. Res. Lett.* **43** 2819–2826, https://doi.org/10.1002/2016GL068036.

Hoell A, Funk C, Zinke J and Harrison L 2017 Modulation of the southern Africa precipitation response to the El Nino Southern Oscillation by the subtropical Indian Ocean Dipole; *Clim. Dyn.* **48(7)** 2529–2540, https://doi.org/10.1007/s00382-016-3220-6.

Holmes C R, Woollings T, Hawkins E and de Vries H 2015 Robust future changes in temperature variability under greenhouse gas forcing and the relationship with thermal advection; *J. Clim.* **29** 2221–2236, https://doi.org/10.1175/JCLI-D-14-00735.1.

Horton R M, Mankin J S, Lesk C, Ethan C and Raymond C 2016 A review of recent advances in research on extreme heat events; *Curr. Clim. Change Rep.* **2** 242–259, https://doi.org/10.1007/s40641-016-0042-x.

Hoy A, Hansel S, Skalak P, Ustrnul Z and Bochnicek O 2017 The extreme European summer of 2015 in a long-term perspective; *Int. J. Climatol.* **37** 943–962, https://doi.org/10.1002/joc.4751.

Kiladis G N and Diaz H F 1989 Global climatic anomalies associated with extremes in the Southern Oscillation; *J. Clim.* **2** 1069–1090, https://doi.org/10.1175/1520-0442(1989)002%3c1069:GCAAWE%3e2.0.CO;2.

Kim M, Lau W K M, Kim K, Jeong S, Kim Y and Lee W 2016 Amplification of ENSO effects on Indian summer monsoon by absorbing aerosols; *Clim. Dyn.* **46** 2657–2671, https://doi.org/10.1007/s00382-015-2722-y.

Kothawale D R and Rupa Kumar K 2005 On the recent changes in surface temperature trends over India; *Geophys. Res. Lett.* **32** L18714, https://doi.org/10.1029/2005GL023528.

Kushnir Y, Seager R, Ting M, Naik N and Nakamura J 2010 Mechanisms of tropical atlantic SST influence on North American precipitation variability; *J. Clim.* **23** 5610–5628, https://doi.org/10.1175/2010JCLI3172.1.

Lhotka O and Kysely J 2015 Hot Central-European summer of 2013 in a long-term context; *Int. J. Climatol.* **35** 4399–4407, https://doi.org/10.1002/joc.4277.

Lu R-Y and Chen R-D 2016 A review of recent studies on extreme heat in China; *Atmos. Sci. Lett.* **9(2)** 114–121, https://doi.org/10.1080/16742834.2016.1133071.

Luo M and Lau N 2017 Heat waves in southern China: Synoptic behavior, long-term change, and urbanization effects; *J. Clim.* **30** 703–720, https://doi.org/10.1175/JCLI-D-16-0269.1.

Mazdiyasni O, AghaKouchak A, Davis S, Madadgar S, Mehran A, Ragno E *et al.* 2017 Increasing probability of mortality during Indian heat waves; *Sci. Adv.* **3** e1700066, https://doi.org/10.1126/sciadv.1700066.

Meehl G A and Tebaldi C 2004 More intense, more frequent and longer lasting heat waves in the 21st century; *Science* **305** 994–997, https://doi.org/10.1126/science.1098704.

Moberg A, Jones P D, Lister D, Walther A and Brunet M 2006 Indices for daily temperature and precipitation extremes in Europe analyzed for the period 1901–2000; *J. Geophys. Res.*, **111(D22106)**, https://doi.org/10.1029/2006JD007103.

Naveena N, Satyanarayana G C, Bhaskar Rao D V and Srinivas D 2021a An accentuated 'hot blob' over Vidarbha, India, during the pre-monsoon season; *Nat. Hazards* **105** 1359–1373, https://doi.org/10.1007/s11069-020-04357-2.

Naveena N, Satyanarayana G Ch, Dharma Raju A, Sivasankara Rao K and Umakanth N 2021b Spatial and statistical characteristics of heat waves impacting India; *AIMS Environ. Sci.* **8(2)** 117–134, https://doi.org/10.3934/environsci.2021009.

Newman M, Alexander M A, Ault T R, Cobb K M, Deser C, Di Lorenzo E *et al.* 2016 The Pacific decadal oscillation, revisited; *J. Clim.* **29** 4399–4427, https://doi.org/10.1175/JCLI-D-15-0508.1.

Nicholls N, Baek H J, Gosai A, Chambers L E, Choi Y, Collins D *et al.* 2005 The El Niño Southern Oscillation and daily temperature extremes in East Asia and the West Pacific; *Geophys. Res. Lett.* **32(16)** L16714, https://doi.org/10.1029/2005GL022621.

Pai D S, Thapliyal V and Kokate P D 2004 Decadal variation in the heat and cold waves over India during 1971–2000; *Mausam* **55(2)** 281–292.

Pai D, Smitha Nair and Ramanathan A 2013 Long term climatology and trends of heat waves over India during the recent 50 years (1961–2010); *Mausam* **64** 585–604.

Pai D, Srivastava A and Smitha Nair 2017 Heat and cold waves over India; In: *Observed climate variability and change over the Indian Region*; (eds) Rajeevan M and Nayak S, Springer, Singapore, https://doi.org/10.1007/978-981-10-2531-0_4.

Parthasarathy B and Dhar O N 1974 Secular variations of regional rainfall over India; *Quart. J. Roy. Meteorol. Soc.* **100** 245–257.

Pezza A, Rensch P and Cai W 2012 Severe heat waves in Southern Australia: Synoptic climatology and large scale connections; *Clim. Dyn.* **38** 209–224, https://doi.org/10.1007/s00382-011-1016-2.

Philander S G H 1983 El Niño Southern Oscillation phenomena; *Nature* **302** 295–301.

Rasmusson E M and Carpenter T H 1983 The relationship between Eastern Equatorial Pacific Sea surface temperatures and rainfall over India and Sri Lanka; *Mon. Weather Rev.* **111** 517–528, https://doi.org/10.1175/15200493(1983)111%3c0517:TRBEEP%3e2.0.CO;2.

Ratnam J V, Behera S, Bishoyi R S, Rajeevan M and Yamagata T 2016 Anatomy of Indian heatwaves; *Sci. Rep.* **6** 24395, https://doi.org/10.1038/srep24395.

Ray K, Chincholikar J R and Mohanty M 2013 Analysis of extreme high temperature conditions over Gujarat; *Mausam* **64(3)** 467–474.

Rohini P, Rajeevan M and Srivastava A K 2016 On the variability and increasing trends of heat waves over India; *Sci. Rep.* **6** 26153, https://doi.org/10.1002/joc.1141.

Ropelewski C F and Halpert M S 1987 Global and regional scale precipitation patterns associated with the El Niño/Southern Oscillation; *Mon. Weather Rev.* **115** 1606–1626, https://doi.org/10.1175/1520-0493(1987)115%3c1606:GARSPP%3e2.0.CO;2.

Roxy M K, Ritika K, Terray P and Masson S 2014 The curious case of Indian Ocean warming; *J. Clim.* **27(22)** 8501–8509.

Roxy M K *et al.* 2015 Drying of Indian subcontinent by rapid Indian Ocean warming and a weakening land-sea thermal gradient; *Nat. Commun.* **6** 1–10, https://doi.org/10.1038/ncomms8423.

Rupa Kumar K, Sahai A, Kumar K, Patwardhan S, Mishra P K, Revadekar J *et al.* 2006 High-resolution climate change scenarios for India for the 21st century; *Curr. Sci.* **9** 334–345.

Rusticucci M 2012 Observed and simulated variability of extreme temperature events over South America; *Atmos. Res.* **106** 1–17, https://doi.org/10.1016/j.atmosres.2011.11.001.

Sandeep A and Prasad V S 2018 Intra-annual variability of heat wave episodes over the east coast of India; *Int. J. Climatol.*, https://doi.org/10.1002/joc.5395.

Satyanarayana G C and Dodla D V 2020 Phenology of heat waves over India; *Atmos. Res.*, https://doi.org/10.1016/j.atmosres.2020.105078.

Srivastava A, Rajeevan M and Kshirsagar S 2009 Development of a high resolution daily gridded temperature data set (1969–2005) for the Indian region; *Atmos. Sci. Lett.* **10** 249–254, https://doi.org/10.1002/asl.232.

Su H, Neelin J and Chou C 2001 Tropical teleconnection and local response to SST anomalies during the 1997–1998 El Niño; *J. Geophys. Res.* **106** 20,025–20,044, https://doi.org/10.1029/2000JD000124.

Trenberth K E 1976 Spatial and temporal variations of the Southern Oscillation; *Quart. J. Roy. Meteorol. Soc.* **102** 639–653.

Webster P J, Magana V O, Palmer T N, Shukla J, Tomas R A, Yanai M and Yasunari T 1998 Monsoons: Processes, predictability, and the prospects for prediction; *J. Geophys. Res.* **103** 14,451–14,510.

Wolter K, Dole R M and Smith C A 1999 Short-term climate extremes over the continental United States and ENSO. Part I: Seasonal temperatures; *J. Clim.* **12** 3255–3272, https://doi.org/10.1175/1520-0442(1999)012%3c3255:STCEOT%3e2.0.CO;2.

Zeng X, Zuo C, Zhang Y, Ning Wang, Zheng Y and Chen C 2017 Feedback between surface air temperature and atmospheric circulation in high-temperature weather in East China: A diurnal perspective; *Atmos. Sci. Lett.*, https://doi.org/10.1002/asl.750.

Yadav R K 2016 On the relationship between Iran surface temperature and north-west India summer monsoon rainfall; *Int. J. Climatol.* **36** 4425–4438, https://doi.org/10.1002/joc.4648.

Zhang X, Alexander L, Hegerl G C, Jones P, Klein Tank A, Peterson T C, Trewin P and Zwiers F W 2011 Indices for monitoring changes in extremes based on daily temperature and precipitation data; *Wires Clim. Change*, https://doi.org/10.1002/wcc.147.

Corresponding editor: T Narayana Rao